AIAA 93-0702
TSS-1: Orbiter Current and Voltage Experiments

D.C. Thompson, W.J. Raitt
Utah State University
Logan, UT
C. Bonifazi
Italian Space Agency
Patrizi, Italy
S.D. Williams, V.M. Aguero
Stanford University
Stanford, CA
B.E. Gilchrist, P.M. Banks
University of Michigan
Ann Arbor, MI

31st Aerospace Sciences Meeting & Exhibit
January 11-14, 1993 / Reno, NV

TSS-1: ORBITER CURRENT AND VOLTAGE EXPERIMENTS

D.C. Thompson, W.J. Raitt
Utah State University, Logan
C. Bonifazi
Italian Space Agency
S.D. Williams, V.M. Aguero
Stanford University
B.E. Gilchrist, P.M. Banks
University of Michigan

Abstract

Although the deployment distance of the TSS-1 tethered satellite was only about 1% of nominal, experiments to study the current collection and vehicle charging effects at low voltages were performed. In this paper we present measurements of Orbiter charging resulting from electron beam emission from the Orbiter, currents in the TSS system with and without electron beam emissions, and the effects of Orbiter thrusters on charging and currents. Generally, charging induced by beam emission was limited to a few volts, though during times with low ambient plasma density the Orbiter was charged up to 80V. Thrusters are seen to enhance Orbiter charging during beam emission, and reduce ion current collection at other times.

Introduction

The first mission of the Tethered Satellite System (TSS-1) was an experiment to demonstrate the feasibility of deploying an instrumented current collecting satellite attached to a 20km length of conducting, insulated wire from the cargo bay of the Space Shuttle. Upward deployment of the satellite and the easterly motion of the Space Shuttle resulted in an induced emf with the polarity being such that the satellite was biased positively relative to the Orbiter. Once the tether was deployed, the overall goals of the mission were to study the dynamics of the deployed system both during deployment and retrieval, and during two station keeping periods; and to perform experiments on electrodynamic effects resulting from the induced emf and the ionospheric connections at each end. The project was jointly funded by NASA and the Italian Space Agency (ASI). The prime contractor for the tether deployment system was Martin Marietta Aerospace Group (MMAG), Denver.

The satellite instrumentation included sensors to study details of the mechanism of current collection at the satellite due to induced emf in the tether as it moved within the geomagnetic field at orbital speed. These measurements were complemented by Orbiter based instrumentation to study the induced emf, the Orbiter potential, provide additional current measurements and to manage the charge collected by the satellite by electron emission from the Orbiter ground or from the tether/satellite directly. In this paper we will concentrate on the measurements from instrumentation to measure tether currents and voltages with varying loads connected between the tether and Orbiter ground with and without electron beam emission drawing the emitted electrons from the frame of the Orbiter. This collection of instruments is known as the Shuttle Electrodynamics Tether System (SETS), and was provided by a consortium of the University of Michigan, Stanford University and Utah State University with the project direction being at Michigan. Measurements of the tether current and the induced emf were also provided by ASI instruments.

Even though the tether was only deployed to about 1% of its planned length, the maximum length of 267m allowed limited studies of the current collecting capability of the system, albeit at relatively low induced emf. We will discuss the results obtained from two different experiments to measure current collecting capabilities of the system and the charging and discharging characteristics of the Space Shuttle Orbiter. Experiments on Space Shuttle Orbiter charge management using electron beam emission to charge the Orbiter had been performed on two previous occasions as part of the Vehicle Charging and Potential (VCAP) experiment flown on STS-3 and STS-51F.[1,2] The deployed satellite during TSS-1 provides a direct measurement of the Orbiter potential relative to the plasma that was not available on either of the VCAP missions.

Circuit Description

The TSS-1 scientific instruments pertinent to this paper, and their connection to other Orbiter systems is shown schematically in Figure 1. Figure 1 also includes the definition of acronyms. The modes of operation of each of the SETS systems were controlled by command sequences generated from the DEP, which in turn was commanded by the SFMDM. The SFMDM also commanded the other science instruments. The preprogrammed sequences were configured to optimize the

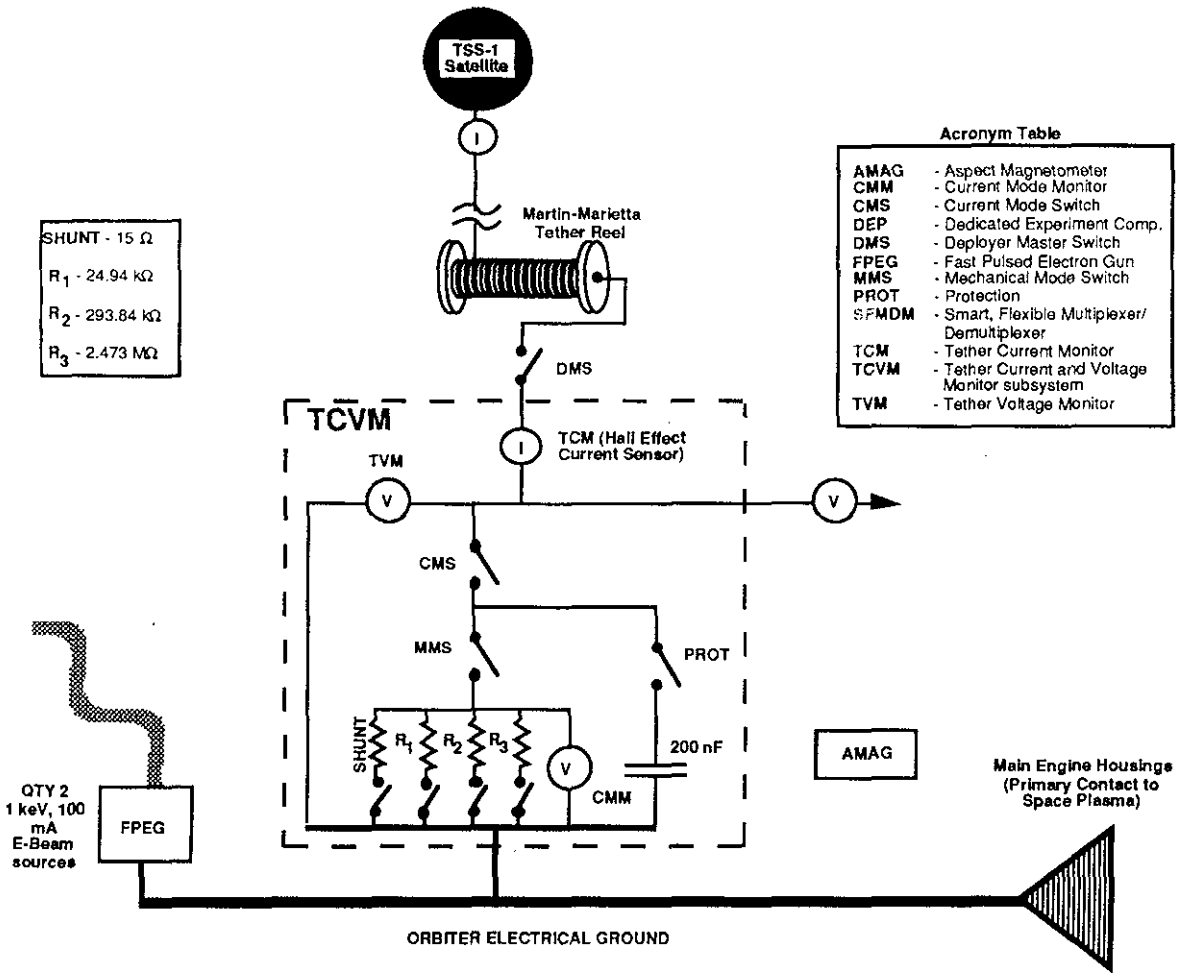

Figure 1. Partial TSS-1 Schematic.

data from all available instruments on both the Orbiter and the satellite.

The heart of the SETS electrodynamic measurement is the TCVM. The major components to control and measure the electrodynamics of the satellite/tether/Orbiter system are shown enclosed in the broken line box in Figure 1. The Orbiter end of the tether is connected to the TCVM through the DMS which is an ASI supplied relay capable of disconnecting the tether with it full induced voltage and a current of 2A. The tether connection then passes through a Hall effect current sensor and is looped out to provide a connection to the ASI measurement of tether voltage and the ASI supplied electron guns, designed to be operated directly from the induced emf in the tether as the accelerating potential. Within the TCVM the tether is connected to a relay/resistor/capacitor network to control the tether/Orbiter ground connection. The indicated voltage and current monitors enable the circuit values to be determined for a variety of modes of the resistor/capacitor combinations.

The FPEG provides the capability of emitting either 100mA or 200mA of electron current from the Orbiter frame by generating a 1kV electron beam. Magnetic orientation of the Orbiter to help determine FPEG beam escape or hit conditions was measured by the AMAG, a 3-axis fluxgate magnetometer.

During nearly all of the deployed operations, the Orbiter was oriented such that the engine bells were in the ram direction and the payload bay was pointing radially away from the earth's center. Since the engine bells provide the main conducting surface connected to the Orbiter frame, this orientation was well suited to complete a current path by ion collection from the ambient ionospheric plasma.

DEP1 Experiment

The DEP1 (abbreviated form of deployment, first orbit) experiment was intended to be performed approximately 15 times during the early deployment phase of the TSS-1 mission. The preprogrammed sequence was intended to take advantage of the relatively low emf available during this time (planned to be less than 500V) as well as the varying distance between the Orbiter and the instrumented satellite. Since there were several attempts to deploy the satellite, and since the satellite was never deployed beyond 267m, the DEP1 experiment was

performed 71 times during deployed operations. DEP1's were by far the most repeated experiment during TSS-1.

Each DEP1 was comprised of four 100s steps. In the first step the FPEG was pulsed at various frequencies and duty cycles, while the satellite was separated from the Orbiter by a high impedance and used as a reference electrode. This was intended to allow measurements of the Orbiter potential relative to the plasma as it varied with the FPEG operational mode, as well as provide an active stimulus to the plasma which could be studied by the instruments on the electrically isolated satellite.

During the second step the FPEG nominally emitted a DC electron beam while the various load resistors were used to connect the tether to the Orbiter electrical ground. The FPEG emission was intended to keep the Orbiter near the plasma potential so that all of the available emf could be used to drive currents in the tether and form an electron collection sheath about the satellite. Since the Orbiter was at a known potential, as determined in the first step, the current-voltage relationship for the satellite could be accurately determined.

The third 100s step of a DEP1 sequence included the same sequence of load resistors as step two, but the FPEG did not emit an electron beam. This step was intended to study the voltage division between the satellite and Orbiter and the ability of the Orbiter to collect an ion current to balance the electrons collected at the satellite.

The fourth step of each DEP1 was entirely passive. That is, the satellite was electrically isolated from the Orbiter and there were no beam emissions from the FPEG. During this step the emf induced by the tether's velocity relative to the geomagnetic field was monitored, and ambient plasma parameters were to be obtained.

DEP1, Step 1: FPEG

The measured potential between the Orbiter and the satellite during the first step of a typical DEP1 during orbital day is shown in Figure 2. The dashed line in the figure is the calculated $v \times B \cdot l$ potential. The first beam emission during this step was a single 210ms pulse at 218/00:25:23, the effect of which can be seen as the approximately 1V spike in the measured data. There were also short beam emissions at 218/00:25:35 (0.82ms), 218/00:25:37 (3.3ms), 218/00:25:39 (13ms), 218/00:25:41 (26ms), 218/00:25:43 (52ms), and 218/00:25:43 (105ms). Only the latter four of these six show any departure from the normal noise of the measurement.

Beginning at 218/00:25:50 the FPEG was commanded to emit a continuous stream of pulses at several hundred Hertz, but with varying duty cycle, see Table 1. Each duty cycle was held for about two seconds.

At 218/00:26:05 FPEG emission duty cycle was lowered to 11% and held at this value until 218/00:26:13 when the beam was emitted in a DC mode. The beam was stopped at 218/00:26:50.

It can be seen in Figure 2 that emitting a 100mA electron beam from the Orbiter induced charging on the order of 1V during this experiment. The magnitude of this charging was dependent on the ambient plasma density, with higher charging events occurring during orbital night. Also, there appear to be two distinct charging/discharging time-constants. The first response of the potential is very quick, possibly less than the 40ms time resolution of the data in the figure. A second time-scale of several seconds is also evident after the beam on/off transitions. The slow divergence of the measured potential from the $v \times B \cdot l$ curve from 218/00:26:20 to 218/00:26:50 is probably due to the varying plasma density (decreasing with increasing time), rather than further Orbiter charging, since the opposite trend is observed (a slow convergence of the two curves) when the plasma density is increasing.

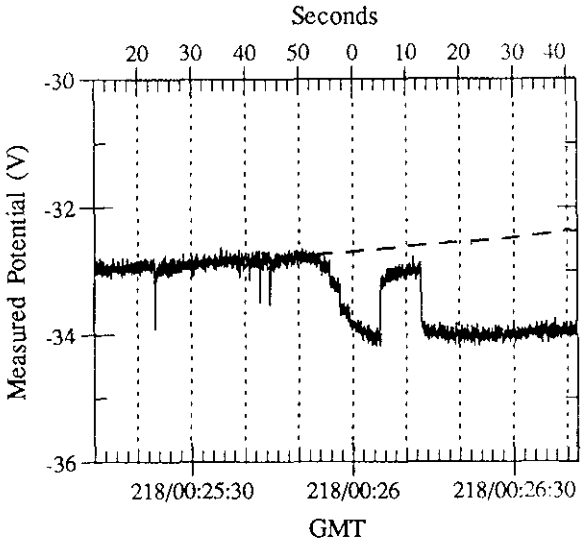

Figure 2. Measured potential and calculated $v \times B \cdot l$ during the first step of a DEP1 sequence, executed during orbital day.

Table 1. FPEG duty cycle variation.

GMT	Frequency	Duty Cycle
218/00:25:50	965	0.1%
218/00:25:52	943	3.2%
218/00:25:54	865	11%
218/00:25:56	650	33%
218/00:25:57	650	67%
218/00:25:59	865	89%
218/00:26:01	943	97%
218/00:26:03	965	99%

The same general features can be seen during the equivalent operation during night (Figure 3). Each FPEG emission during this experiment induces more charging than the corresponding pulse during the day. And the DC

emissions yield an Orbiter potential of approximately 3V from the ambient.

There appears to be no dependence of the charging level obtained during beam emission on whether the primary beam escapes or strikes the Orbiter on its mostly non-conducting surfaces. Further investigation will be required to determine if the charging is reduced when the beam strikes a conducting surface.

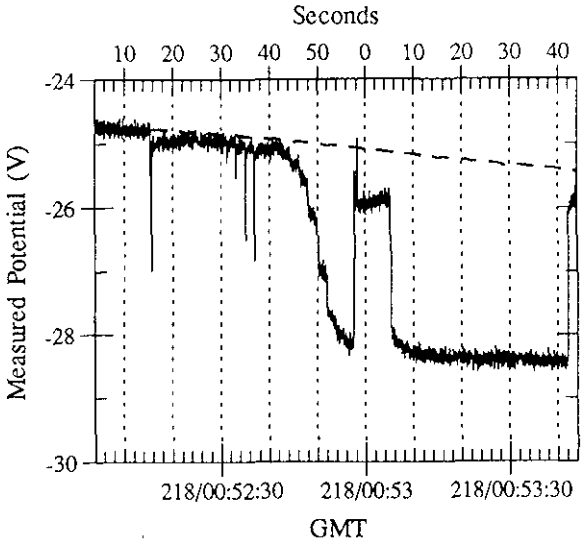

Figure 3. Measured potential and calculated $v \times B \bullet l$ during the first step of a DEP1 sequence, executed during orbital night.

DEP1, Step 2: TCVM and FPEG

The measured voltage and tether current during the second step of a typical daytime execution of the DEP1 sequence is shown in Figure 4. The dashed line through the voltage plot is again the calculated $v \times B \bullet l$ emf. The dashed line through the current plot is the maximum current that could be driven through the tether by the available emf,

$$I_{\max} = \frac{v \times B \bullet l}{R_{\text{tether}}}$$

where the tether resistance is assumed to be 2000Ω.

The FPEG began to emit a DC beam of electrons at 218/00:20:13 and continued in this mode until 218/00:20:48. Each of the TCVM load resistors was used in turn to connect the tether to the Orbiter ground. The 2.5MΩ resistor was engaged first at 218/00:20:21. The impedance of this resistor is large compared to any of the other elements in the circuit (satellite sheath, tether resistance, Orbiter sheath) so no effect is seen when it was used. The spike in voltage at 218/00:20:20 is coincident with Orbiter RCS thruster activity. The effect of Orbiter thrusters on potential will be addressed later in this paper. The 250kΩ resistor was connected at 218/00:20:36 and disconnected at 218/00:20:48. As with the 2.5MΩ resistor, the 250kΩ resistor is much larger than the other resistances in the circuit and so its effect on the voltage measurement was slight, and there was no measurable current. The 25kΩ resistor was engaged from 218/00:20:50 to 218/00:21:02. The change in the measured voltage when the 25kΩ resistor was connected is large enough that we can use it, and the other elements of the circuit, as a voltage divider to estimate the total impedance of the remaining elements. That is,

$$\frac{R_{25k}}{\phi_{25k}} = \frac{R_{\text{other}}}{\phi_{\text{open}} - \phi_{25k}}$$

Or,

$$R_{\text{other}} = \frac{25000(35.5 - 32.7)}{32.7} = 2140\Omega$$

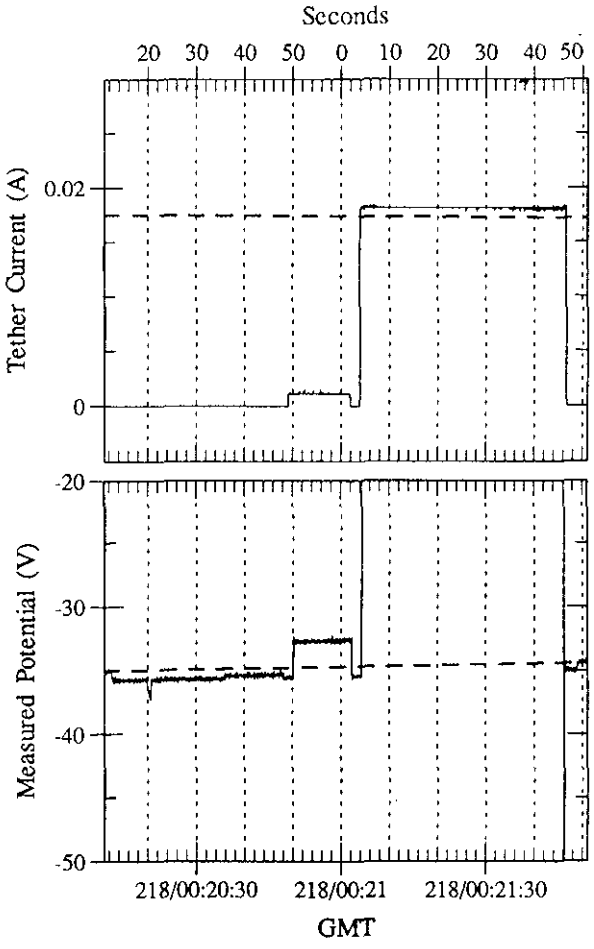

Figure 4. Current and voltage during the second step of a DEP1 sequence, executed during orbital day.

The shunt resistor was connected from 218/00:21:04 to 218/00:21:46. The measured voltage at this time was

essentially zero, being the current multiplied by the resistance of the shunt,

$$\phi = 0.018\text{A} \times 15\Omega = 0.27\text{V}$$

The tether current was higher than the dashed line, I_{max}, since the FPEG had changed the Orbiter potential by about 1V, thereby increasing the available voltage to drive the tether current. Since the shunt resistance is negligible we can calculate the impedance of the other circuit elements by simply dividing the available voltage by the tether current,

$$R_{other} = 36 / 0.018 = 2000\Omega$$

The spike in the measured voltage at the opening of the shunt is due to the inductance of the tether, still mostly wound on a reel.

With few exceptions the features in Figure 4 are seen in both day and night executions of DEP1 cycles. That is, during FPEG beam emissions the current in the tether was limited by the load resistor when the 2.5MΩ, 250kΩ, and 25kΩ resistors are used. And the tether current was limited by the tether resistance when the shunt is engaged. In general, since the induced voltages during TSS-1 were very low compared to the design specifications of the instrumentation, the main impedance in the circuit is the instrumentation itself.

However, there are a few exceptions. The most extreme of these is shown in Figure 5. The measured potential is seen to diverge from about 3V different from $v \times B \cdot l$ at 218/01:00:30, to nearly 7V at 210:01:01:18, after which the shunt was engaged and no further voltage measurement could be made. The tether current, in contrast to the case in Figure 4, was not constant at a level slightly above the I_{max} curve. Rather, it fell from the expected value of approximately 16mA to 8mA just before the shunt was disengaged. After the shunt was removed from the circuit valid voltage measurements were again obtained. Since there was essentially no current in the tether we can assume that the satellite was near plasma potential. Then the difference between $v \times B \cdot l$ and the measured voltage was the Orbiter potential,
-32V - (-112V) = 80V.

We can use a voltage divider argument similar to that used previously to estimate the resistance of elements in the circuit. If we use the tether as the known resistance, and the potential drop in the tether just before the shunt was disengaged as the voltage with the resistor in the circuit, then

$$R_{other} = \frac{2000(112 - (0.008)\ (2000))}{(0.008)\ (2000)} = 12\text{k}\Omega$$

which is six times large than the impedance of the instrumentation. This large resistance was most likely due to a very low ambient plasma density.

Since the 8mA of current in the tether is small compared to the 100mA of the electron beam the potential of the Orbiter was probably not greatly affected by the removal of the shunt from the circuit at 218/01:02:02.

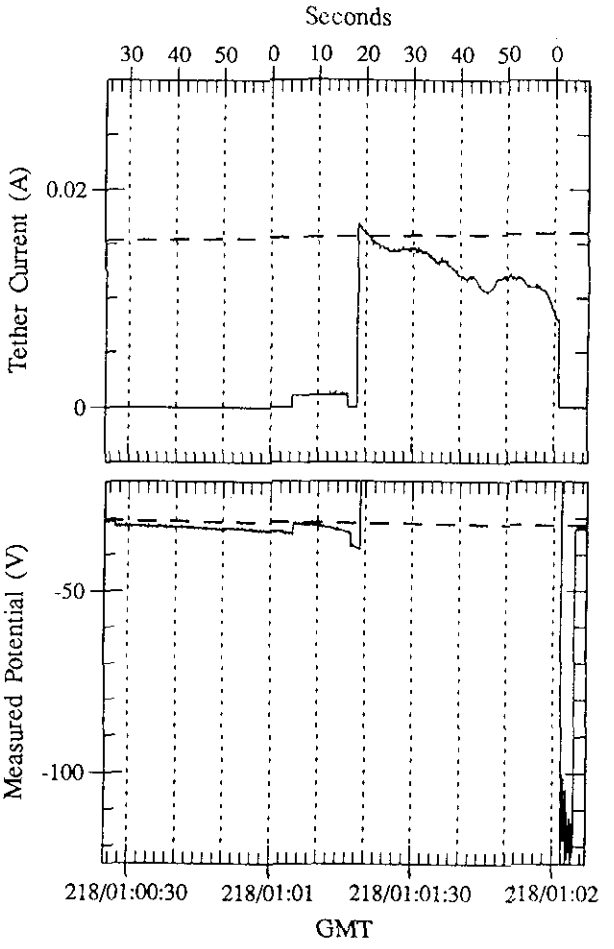

Figure 5. Current and voltage during the second step of a DEP1 sequence, executed during orbital night.

With this assumption we can estimate the potential of the satellite by requiring that all the voltages in the circuit add to zero. That is,

$$\phi_{orbiter} + I_{tether} R_{tether} + \phi_{satellite} + \phi_{measured} = 0$$

Or,

$$\phi_{satellite} = -80 - 0.008 \times 2000 + 112 = 16\text{V}$$

This value is only approximate and the voltages and currents during this time are changing rapidly. But, the potential of the satellite relative to the ambient plasma should be on this order. There were instruments on the satellite that were capable of making this measurement.

DEP1, Step 3: TCVM

During the third step of DEP1 cycles the load relays in the TCVM were used to connect the tether to the Orbiter ground in the same order as they were in the second step. However, the third step was performed without the FPEG electron beam emission to neutralize the Orbiter. There are several occurrences during daytime executions of DEP1, as in Figure 6, wherein the tether current matched very closely the limit imposed by the tether resistance. During these times the ram ion current to the shuttle's engines was sufficient to neutralize the current driven by the $v \times B \cdot l$ potential.

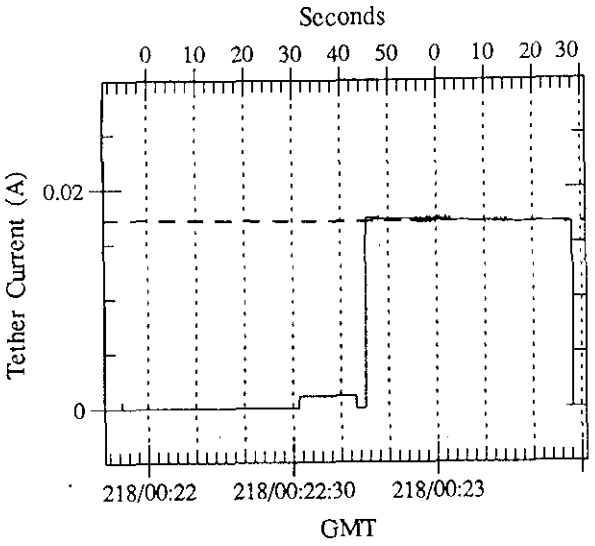

Figure 6. Tether current during the third step of a DEP1 sequence, executed during orbital day.

More typical, however, is a current profile as shown in Figure 7. In this case, the current drawn when the 25kΩ resistor was used was still limited by the 25kΩ, so that other impedances in the circuit were comparatively small. But when the shunt was engaged the tether current was significantly reduced from the $v \times B \cdot l / R_{tether}$ limit. Since the satellite was able to collect more current than this (as evidenced in the second step of the DEP1) it must have been that the ion current to the Orbiter was less than that required to discharge the tether current. Then the Orbiter charged until a current balance was achieved.

The structure in the tether current, seen in Figure 7 after 218/02:43:15, is common to many of the DEP1 executions, and is probably due to fluctuations in the density of the ambient plasma.

When the shunt opens at 218/02:43:30, and after the initial spike in the measured voltage from the tether inductance, the Orbiter is seen to have been charged to about 30V. The Orbiter then discharges and the measured voltage approached the $v \times B \cdot l$ value.

Shunter Experiment

During one orbit of TSS-1 deployed operations, from about 218/10:46 to 218/12:18, the shunt was repeatedly connected for 58s then disconnected and open-circuit voltages were measured for 2s. The FPEG was not operated during this time, nor were any other load resistors engaged. This period of TSS-1 has been referred to as "shunter".

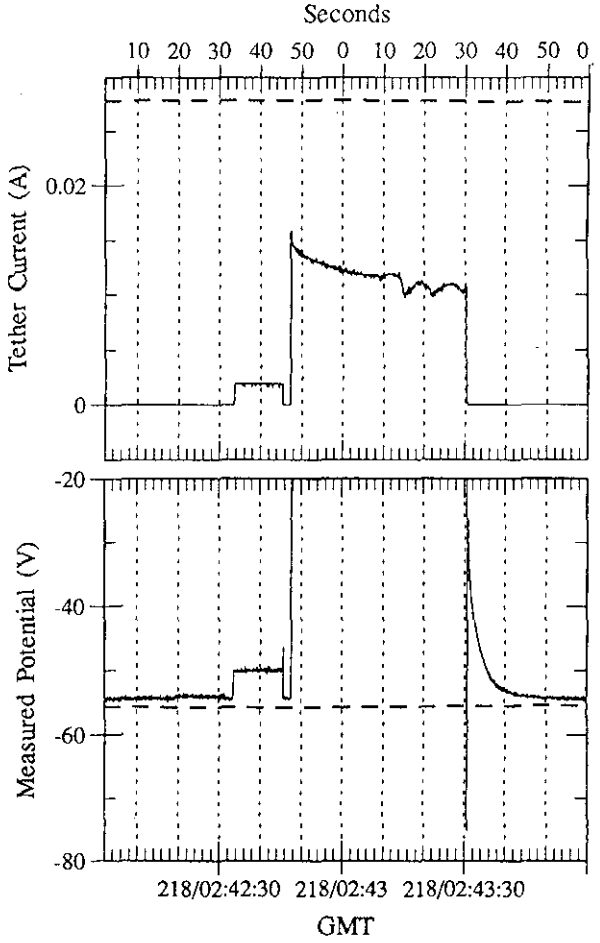

Figure 7. Tether current during the third step of a DEP1 sequence, executed during orbital night.

Figure 8 shows the measured tether current during shunter including the 2s voltage monitoring periods, during which the measured current is zero. Again, $I_{max}=v \times B \cdot l / R_{tether}$ is plotted in the figure as a dashed line. I_{max} is seen to be the upper limit on tether current during much of the orbital day. However, during part of the orbital day, particularly the morning, and through the orbital night, the current is smaller than I_{max}. The spikes at the closure of the shunt relay evident through much of the orbit are a result of the capacitance between the Orbiter and the plasma.

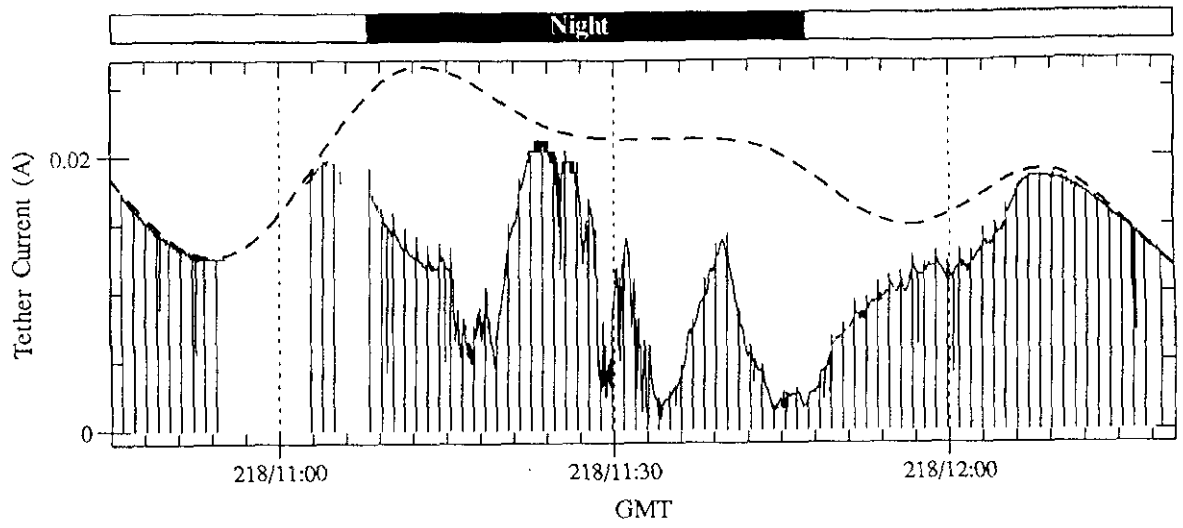

Figure 8. Tether current during the shunter experiment.

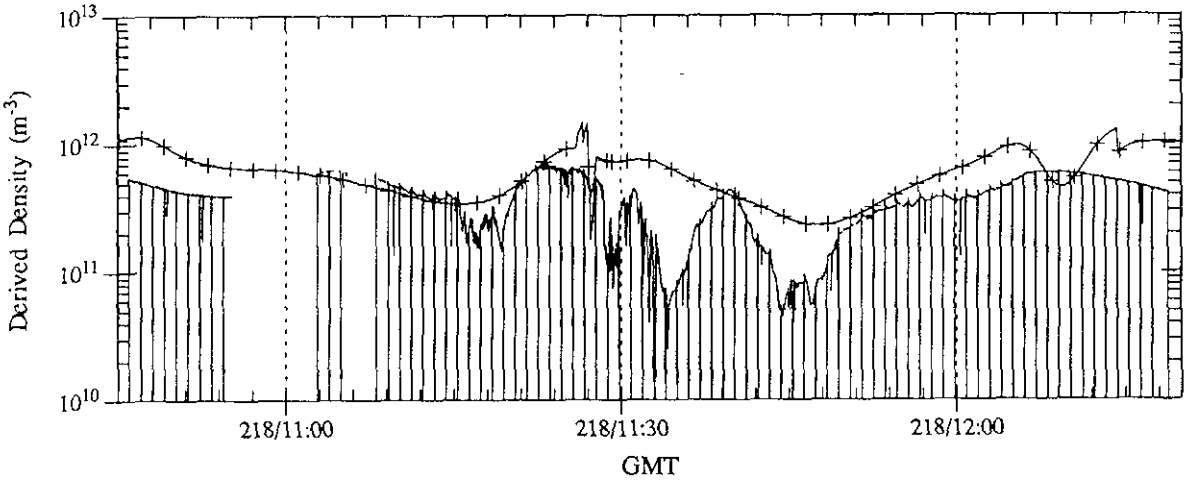

Figure 9. Derived plasma density during the shunter experiment.

The Orbiter is moving with a supersonic velocity with respect to the ambient ions. If we assume an effective collecting area, A, then the current that the uncharged Orbiter can collect is given by,

$$I_{\text{orbiter}} = Anqv$$

where n is the plasma density, q is the magnitude of the electronic charge, and v is magnitude of the Orbiter velocity with respect to the plasma. Since the Debye length is small compared to the primary current collecting surface area on the Orbiter (the main engines) the effective area should not increase by a large factor as a result of the limited charging events during shunter. Rather, as the potential of the Orbiter is raised the potential across the tether is reduced, thereby reducing the current in the tether. If we ignore the spikes after the relay closure due to the Orbiter capacitance then $I_{\text{orbiter}} = I_{\text{tether}}$. So, we can invert to obtain a derived density,

$$n = \frac{I_{\text{tether}}}{Aqv}$$

Figure 9 shows the derived density and the plasma density predicted by the IRI ionospheric model,[3] which is the curve marked by + symbols. The effective collecting area of the Orbiter is not accurately known, but is thought to be about 25m^2, which is the value used for this paper.

Anytime that the resistance of the tether limited the current flow, that is, anytime that the current was near I_{max}, the derived density is clipped at an artificially low level. However, during a large portion of the shunter orbit the tether did not reduce the tether current. During those times the derived density in Figure 9 should reflect the actual plasma density. Note the rapid variation and

detailed structure of the derived density, which IRI would not be expected to predict.

Thruster Effects

Figures 10, 11 and 12 show the effects that Orbiter RCS thrusters have on the TSS-1 current/voltage system for the three operating modes discussed in this paper. At this writing the data on thruster activity is limited to 1Hz and no information about which of the several Orbiter thrusters were actually firing is available. This information was recorded and when it becomes available will be used to quantify the effects of different thrusters, and the time variation of potentials an currents during thruster operation.

At the time shown in Figure 10, the FPEG was emitting a DC electron beam while the tether/satellite was used as a reference. The thruster was operating from about 218/00:33:03 to 218/00:33:08. Before the thruster activity the Orbiter potential was close to 2V positive compared to the local plasma potential. The potential is seen to become more positive coincident with the thruster operation, rising to 20V in this case. The potential falls rapidly back to a level near the pre-thruster value very quickly after the end of the thruster firing.

The gases from the thruster evidently inhibited the collection of electrons by the Orbiter, which was necessary to offset the current emitted by the beam. Hence the Orbiter must have charged positively until current balance was achieved.

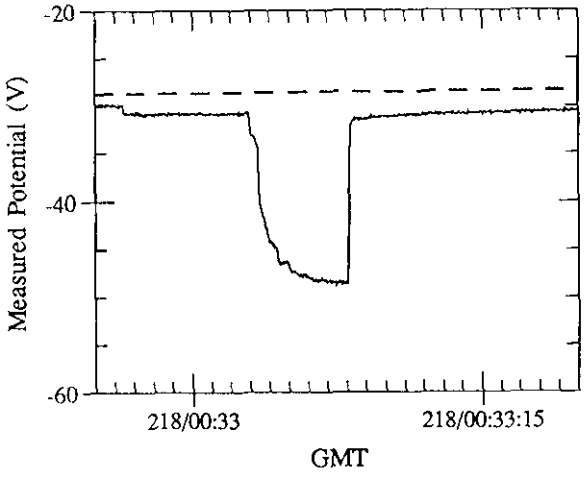

Figure 10. Orbiter thrusters during FPEG emission.

When thruster activity occurred in conjunction with tether current (shunt engaged) and FPEG emission, as in Figure 11 from 218/00:27:49 to 218/00:27:54, the tether current is seen to be enhanced relative to the current without thrusters. Since the thruster cannot change the tether resistance, the only way to drive more current in the tether was to increase the applied voltage, by allowing the FPEG to charge the Orbiter positively as in Figure 10. We can estimate the change in Orbiter potential from the change in tether current,

$$\Delta\phi_{\text{orbiter}} = \Delta I_{\text{tether}} R_{\text{tether}} \cong 0.005(2000) = 10\text{V}$$

Thruster activity occurring during times when the shunt was engaged but the FPEG was not operating reduce the tether current. For example, Figure 12 shows the current for such a case with thrusters active from 218/00:43:00 to 218/00:42:02 and again from 218/00:42:04 to 218/00:42:10. In this mode the thrusters seem to have reduced the ion current to the Orbiter. For current balance to be maintained the Orbiter must have charged negatively to limit the tether current,

$$\Delta\phi_{\text{orbiter}} = \Delta I_{\text{tether}} R_{\text{tether}} \cong -16\text{V}$$

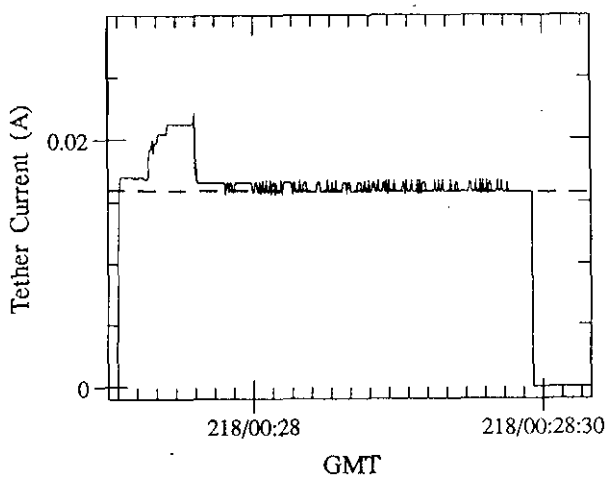

Figure 11. Orbiter thrusters with FPEG and tether current.

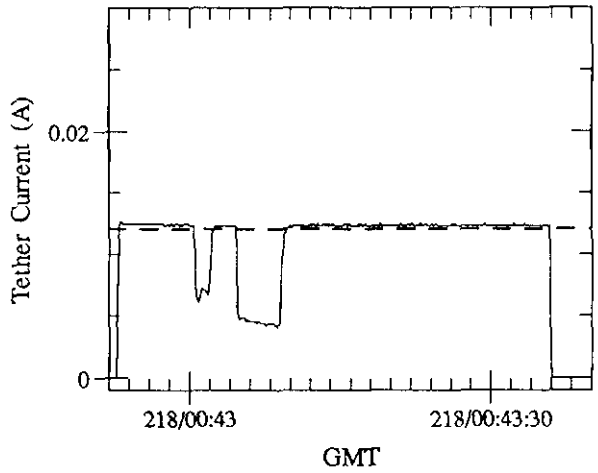

Figure 12. Orbiter thruster effect on tether current without FPEG.

Summary

The much reduced deployment length of the tether from what was planned for the TSS-1 mission prevented the prime scientific objectives of the mission being achieved. However, the deployment length was sufficient that a number of interesting electrodynamic experiments were able to be performed. In this paper we have reported on results which provided information on the induced voltages in the short tether, and the currents driven through different circuit impedances and different connections of the tether to the ionosphere at the Orbiter end.

In the passive voltage monitoring mode the induced emf was measured to be coincident to the value predicted by Faraday's law. The operation of the FPEG allowed a direct measurement of the electrical potential to which the Orbiter was driven to collect sufficient electrons to balance the electron emission current from the FPEG. The potential was strongly dependent on the ambient ionospheric density, varying from about 1 volt during daytime conditions to about 80 volts during nighttime depleted ionospheric density conditions.

Experiments in which differing impedances were connected into the tether circuit demonstrated that in daytime conditions the largest impedance in the complete circuit was the 2000Ω resistance of the tether wire itself whether the FPEG was operating or not. However, during low ionospheric plasma density conditions, the sheath impedances were observed to increase to as much as 12kΩ in one case.

The experiment was also configured to allow the study of the effect of gas release from the Orbiter attitude control system. It was found that the release of the gas in all cases studied resulted in Orbiter potential changes or return ion current changes that were consistent with a depletion of the ambient ionospheric plasma density induced by the gas release.

There was no opportunity during TSS-1 to perform the joint experiments planned to incorporate the entire instrument complement in coordination. The small sample of results presented in this paper show that even with the short tether deployment, the TSS-1 mission would have yielded a great deal of valuable data on the science and engineering aspects of the electrodynamic interaction of tethered systems with the LEO space environment. The electrodynamic validity of TSS-1 experiments directed to those studies showed that there is great promise for a significant gain in knowledge as the induced emf is increased to greatly exceed the ionization potentials of ambient and contaminant gases, and current densities to exceed the thresholds for plasma instabilities. We strongly support a reflight of the existing equipment, and hope that this can be accommodated in the NASA and ASI programs.

References

1. Banks, P.M., W.J. Raitt, A. B. White, R.I. Bush, and P.R. Williamson, *Results from the Vehicle Charging and Potential Experiment on STS-3*, AIAA J. Spacecr. Rockets, *24*, 138,1987.
2. Hawkins, J.G., *Vehicle Charging and Return Current Measurements during Electron Beam Emission Experiments from the Shuttle Orbiter*, Ph.D. Dissertation, Stanford Univ., Stanford, CA, 1988.
3. Rawer, K., S. Ramakrishnan, D. Bilitza, *International Reference Ionosphere 1978*, URSI Brussels and World Data Center, Report UAG-82, Boulder, 1981.

Acknowledgments

This work was funded by NASA under contracts NAS8-39381 to the University of Michigan and NAS8-36812 to Stanford University, with subcontracts from those institutions to Utah State University.

The authors express gratitude to Marilyn Oberhardt and David Hardy of the USAF Phillips Laboratory for their assistance in acquiring and analyzing the data used in this paper. The contributions of P.R. Williamson and A.B. White during instrument development is acknowledged with appreciation.